Calculation of Low Mach Number Reacting Flows

Harry A. Dwyer*
University of California, Davis, Davis, California

A numerical method has been developed to calculate low Mach number and reacting flows in general and the burning and vaporization of a hydrocarbon droplet in particular. The method is time accurate and it makes use of the continuity equation to form a pressure correction. The basic transport equations have been given a finite-volume form, and a predictor/corrector algorithm has been employed. The continuity equation and the pressure-correction step have been solved to high numerical accuracy with the use of direct solver technique, which also has the advantage of improved efficiency. The physical problem of the burning and vaporization of a high molecular weight hydrocarbon droplet is a very difficult one due to the very large temperature and density gradients in the flow, and also due to the complicated flow structures which develop during a droplet's lifetime. The methods used in this research have successfully solved these problems, and a detailed history of the droplet has been calculated and studied.

Introduction

THE purpose of this article is to describe the progress that has been made in the numerical simulation of the unsteady processes that occur during the vaporization and combustion of individual hydrocarbon fuel droplets in a hot oxidizing environment. It is the premise of this type of research that a good understanding of the most important physical processes in droplet dynamics can be obtained with a digital computer simulation, and that the studies will be valuable in other areas of combustion science such as spray combustion. It is also the purpose of the article to describe the methods that have been used in detail so that they can be utilized and improved as the power of the digital computer grows.

Although there has been a large number of developments in the use of the digital computer to simulate many fluid-flow problems in such fields as aerodynamics and simple turbulent flow, there has not been as much activity in multiphase and reacting flows. The primary reason is due to the fact that a vaporizing and burning droplet involves the interplay of a large number of different physical time scales. These time scales are characterized by the dimensionless parameters which appear in the equations of motion and are well-known by the names of the famous men who have contributed to their use, such as Reynolds, Domkohler, Mach, Prandlt, and Lewis. The resulting difficulties from the multiple time scales in reacting flow problems can be comprehended when one is reminded of the fact that many gifted scientists spent their entire careers in studying only a small portion of the time-scale variation associated with just one dimensionless parameter, such as Reynolds number.

An early and current leader in low Mach number flows has been the group at Imperial College in London under the original leadership of Brian Spalding, which has developed a large number of outstanding researchers. A good survey of the present state of the methods, which have been used to solve a wide variety of reacting and nonreacting flows, can be found in the textbook of Patankar.[1] A more general view of the development of the field can be found in the pioneering textbook of Roache,[2] and this book describes in detail many of the early research efforts at Los Alamos National Laboratories and the efforts by Chorin.[3] The problems that developed in the solution of low Mach number flows were due to a sensitivity to errors in the calculation of the pressure field from the continuity equation, and a possible decoupling of the pressure field from the velocity field if certain types of difference schemes are utilized. It is known that there are many ways to avoid these problems, and a modern new approach will be presented in this article.

One of the first numerical efforts to study the vaporization of a hydrocarbon droplet was the steady-state work of Renksizbulut.[4] In this investigation, a steady-state correlation for the total drag and Nusselt number was investigated and compared with experimental results and found to have merit. Unsteady investigations of vaporizing hydrocarbon droplets were carried out by Dwyer and Sander,[5,6] with an averaged-density approximation. Further and more complete studies by Patnaik, et al.[7] and Haywood[8] confirmed these results, and the investigation of Haywood showed that a modified form of the steady-state correlation of Renksizbulut may have validity in complex hydrocarbon studies.

Problem Definition

A description of the physical problem to be addressed is exhibited in Fig. 1 where the flow over a vaporizing droplet is shown in a schematic way. As can be seen from this figure, the flowfield is characterized by the freestream conditions far from the surface and upstream, the droplet itself and its interface, and the conditions downstream and far from the surface. In its most complete form, the problem involves an interaction between gas and liquid phases, and the complete system must be modeled and calculated. The basic tasks are made much more difficult for the burning of hydrocarbon fuel droplets because of the very large variation of physical and transport properties which occur due to differences in species molecular weight and the large temperature differences caused by chemical reactions and freestream conditions. An example of typical property variations caused by individual effects for a decane droplet is presented in the lower portion of Fig. 1. If the cold surface characteristics of pure decane are used for the density and the viscosity rather than the hot-gas freestream properties, the Reynolds number varies by more than a factor of 50 times. This variation in Reynolds number is very large and presents serious problems if an approximate calculation of drag and heat transfer is attempted with a semiempirical correlation.

Presented as Paper 88-0640 at the AIAA 26th Aerospace Sciences Meeting, Reno, NV, Jan. 11-14, 1988; received May 16, 1988; revision received April 27, 1989.

*Professor. Department of Mechanical Engineering. Member AIAA.

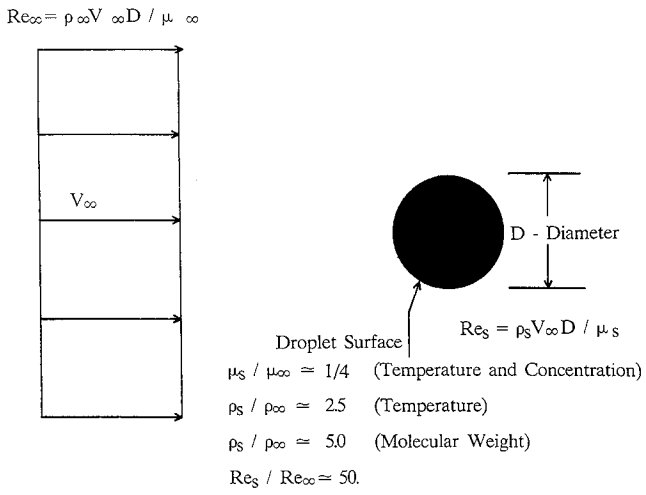

Fig. 1 Flow system and geometry.

System Equations

A very significant finding of this research effort is the importance of the use of control-volume techniques to generate the basic system of finite-difference equations for mass, momentum, and energy transport. It has been the experience of the present investigator that a large number of mistakes are continually being made in going from the differential equations to a finite-size volume when one is trying to describe a complex flow system. A much more physically satisfying approach, and one which leads to a reduced number of errors, is to start with the basic laws of physics written in finite form or the so-called control-volume form. The transport equations in control-volume form can be written as

Continuity Equation:

$$\partial/\partial t[\iiint_v \rho \mathrm{d}V] + \iint_s \rho \boldsymbol{V}\cdot\mathrm{d}\boldsymbol{A} = 0 \tag{1}$$

Momentum Equation:

$$\partial/\partial t[\iiint_v \rho \boldsymbol{V}\mathrm{d}V] + \iint_s \rho \boldsymbol{V}\boldsymbol{V}\cdot\mathrm{d}\boldsymbol{A} = -\iint_s p\,\mathrm{d}\boldsymbol{A} - \iint_s \tau''\cdot\mathrm{d}\boldsymbol{A} \tag{2}$$

Energy Equation:

$$\partial/\partial t[\iiint_v \rho e\,\mathrm{d}V] + \iint_s \rho h\boldsymbol{V}\cdot\mathrm{d}\boldsymbol{A} = -\iint_s \boldsymbol{q}_e\cdot\mathrm{d}\boldsymbol{A} + \iiint_s \rho S_e''\,\mathrm{d}V \tag{3}$$

Species Equation:

$$\partial/\partial t[\iiint_v \rho Y_k\,\mathrm{d}V] + \iint_s \rho Y_k\boldsymbol{V}\cdot\mathrm{d}\boldsymbol{A} = -\iint_s \boldsymbol{q}_k\cdot\mathrm{d}\boldsymbol{A} + \iiint_v \rho S_k''\,\mathrm{d}V \tag{4}$$

where the surface $\mathrm{d}\boldsymbol{A}$ and volume integrals $\mathrm{d}V$, are defined by the midpoints between cells, t is the time, ρ is the density, $\boldsymbol{V}$ is the velocity vector in Cartesian form, τ'' is the stress tensor, $\boldsymbol{q}_e$ is the heat-flux vector, S_e is the heat-release source term, Y_k is the mass fraction of species, $\boldsymbol{q}_k$ is the diffusion flux of species k, and S_k is the chemical rate term for species k.

For problems with moving boundaries, liquid/gaseous interfaces, and complex geometries, the finite-volume formulation offers definite advantages over most other methods due to the physical clarity of the method and its inherent advantage for conservation of physical properties. The method also can treat basic shapes other than generalized quadrilaterals, and it can easily utilize triangular geometries or other useful cell shapes. It can be said that the finite-volume method is the most useful extension of the generalized coordinates methods that have been employed for the development of adaptive gridding and advanced airfoil geometries.[9,10]

The Low Mach Number Limit

For the problems which will be treated in this article, it will be useful to take the low Mach number limit of the above equations. A clear description of this process can be found in the article by Merkle and Choi,[11] and the primary purpose of taking this limit is to eliminate acoustic wave propagation from the system of equations. The result of this process is that the pressure field can be separated into a thermodynamic part, P_r, and a dynamic part, p, which appears in the momentum equations. The thermodynamic part of the pressure is constant in space, and is utilized in the equation of state to calculate the local density for a gas. (For an incompressible fluid, the thermodynamic pressure does not appear directly in the basic equations.) The dynamic part of the pressure field is needed for the solution of the momentum equations, and the lack of an explicit equation to calculate this pressure field has been one of the principal difficulties with this limit of the Navier-Stokes equations.

Most of the methods of the calculation of the dynamic pressure field have been based on the use of the continuity equation to generate an elliptic Poisson equation. The pioneers in this field have been the researchers at the Los Alamos Research Laboratories and A. J. Chorin,[2,3] and the researchers at Imperical College have introduced many variations to the basic methods. Although there has been a significant number of problems solved, there does not seem to be a large amount of effort spend on time-dependent or variable-density problems. In the present paper, a time-dependent method will be given, and many of the difficulties associated with this model in the past will be explained.

Another good reason to utilize the low Mach number model is due to the large temperature differences in a problem with chemical reactions and heat transfer. Local errors in the temperature field of just a couple of degrees centrigrade can be converted into rather large pressure changes when compared to the stagnation pressure for a flow with a maximum velocity of less than 10 m/s. (The reader can check this with the use of the isentropic equations of gas dynamics.) When the low Mach number approximation is applied, this possibility is eliminated since the thermodynamic pressure is constant in space.

Boundary Conditions

The application of boundary conditions is made much simpler with the use of the control-volume formulation of the basic equations. The boundary conditions can usually be obtained by taking the limit as the volume of a cell approaches zero, and by applying results from physical observation. For example, the conditions of a continuous distribution of velocity, temperature, and other thermodynamic variables follow from physical considerations and observations, whereas the conditions for the pressure field, the stresses, the heat fluxes, and the mass fluxes at the interface locations can be found from the surface limit of the control-volume equations.

Numerical Methods

A basic purpose of the article is to present in detail the numerical methods that have been developed and used to solve the present class problems. The challenging droplet-dynamics problem represents a severe test for the numerical methods. The methods used can be described in three parts, and these are given below.

A. Basic Numerical Method

The fundamental philosophy that was considered in the choice of the numerical method was to employ the most implicit method possible within the capability of the memory and speed of the digital computer. The direct solution of the entire system of resulting algebraic equations with a banded solver[12] is a very implicit and accurate method, but is beyond the capability of even the future generation of digital computers

for multidimensional problems with chemical reactions and time-dependent conditions. The first choice considered was the approximate factorization methods developed at NASA Ames,[13] and which are used widely in the Aerospace industry under high Reynolds number conditions. These methods have good stability characteristics for two-dimensional problems and can employ a variety of time-accurate forms; however, they do have some problems with complex grids for lower Reynolds numbers. A better alternative for problems with strong diffusion or elliptic influences is to use predictor/corrector methods with the updating of all of the terms in the equations.[14]

In order to achieve a factored form for the space coordinates, a predictor/corrector two-step algorithm is utilized to solve the convective space terms and the Laplacian-like operators. On the predictor step one coordinate direction is implicit, and on the corrector step the other coordinate direction is made the implicit one. During both steps the new values of T at time $(n + 1)$ are used immediately in the algorithm after being calculated. The finite-difference forms for the diffusion operator on a uniform grid are as follows:

Predictor – x-Direction Implicit:

$$\nabla^2 T = (T^{n'+1_{i+1,j}} - 2T^{n'+1_{i,j}} + T^{n'+1_{i-1,j}})/\Delta x^2 + (T^{n_{i,j+1}} - 2T^{n'+1_{i,j}} + T^{n'+1_{i,j-1}})/\Delta y^2 \quad (5)$$

Corrector – y-Direction Implicit:

$$\nabla^2 T = T^{n'+1_{i+1,j}} - 2T^{n+1_{i,j}} + T^{n+1_{i-1,j}})/\Delta x^2 + (T^{n+1_{i,j+1}} - 2T^{n+1_{i,j}} + T^{n+1_{i,j-1}})/\Delta y^2 \quad (6)$$

where the index $(n' + 1)$ denotes the predicted values from the first part of the algorithm.

The main advantage of a predictor/corrector algorithm is for problems with large differences in grid cell or fast chemistry. In this situation, the added implicitness of the corrector and the updating of all terms in the equation can make a substantial improvement in the efficiency and stability of the resulting solution. (There is some degradation of time accuracy for the predictor, but this can be improved with an ADI type of predictor.) An example of this improvement for a complex grid system is shown in Figs. 2 and 3, where the convergence histories of three algorithms are given for a skewed and stretched grid. The time step taken in the numerical simulation was equal to the value for a purely explicit method on the largest grid cell, but this step is much larger than the explicit time step for the fine cells near the origin (actually 1000 times larger). The convergence history of the approximate factorization method[13] is poor, whereas the predictor/corrector method compares favorably with the best of all methods, the direct solution of the linear system equations. The reader may be tempted to think that Laplace's equation may not be representative of reacting flow problems, but it must be remembered that both the calculation of flame propagation and the solution of the pressure field are dominated by the Laplacian operator term.

The application of the above algorithm to the finite-volume form of the Navier-Stokes is straightforward but tedious, and can be illustrated with the heat-flux term in the energy equation:

$$-\iint q_e \cdot dA = k(\partial T/\partial x)dA_x + (\partial T/\partial y)dA_y + (\partial T/\partial z)dA_z \quad (7)$$

If the control volumes are defined by a nonorthogonal distribution of cell centers organized with the generalized coordinates ξ, η, and ζ, the above expression becomes

$$-\iint q_e \cdot dA = k[(\partial T/\partial \xi)\xi_x + (\partial T/\partial \eta)\eta_x + (\partial T/\partial \zeta)\zeta_x]dA_x + [(\partial T/\partial \xi)\xi_y + (\partial T/\partial \eta)\eta_y + (\partial T/\partial \zeta)\zeta_y]dA_y + [(\partial T/\partial \xi)\xi_z + (\partial T/\partial \eta)\eta_z + (\partial T/\partial \zeta)\zeta_z]dA_z \quad (8)$$

where a local coordinate transformation issued to between the $x\,y\,z$ and the $\xi\,\eta\,\zeta$ coordinate directions. (This transformation is always found by numerical methods.) The predictor/corrector algorithm is then utilized along the directions ξ, η, and ζ, if the grid points are set up in an ordered fashion. The other terms in the control-volume equations which involve derivatives, such as the stress tensor and the diffusions fluxes, are evaluated in a similar way.

A brief discussion will now be presented for the numerical treatment of the various terms which appear in the basic system of equations. The general rule is that all volume terms are evaluated at the center of the cell, and all surface terms at the surface of cell (the transport properties included). The surface terms can only be found by averaging between cell centers, and for a second-order method (in the finite-difference sense) this implies a linear variation between cell centers. For the convective-flux terms and the pressure force in the momentum equations, there is no coordinate transformation necessary to calculate there terms and only vector dot products are required to form the system of algebraic equations. The major problem that one faces is the calculation of the pressure field from the continuity equation and the sensitivity of the momentum equations to errors in the pressure field. This type of sensitivity is not encountered in high Mach number flows where there seems to be no need to take special precautions. However, for low Mach number flows with or without density variation, special precautions must be taken to avoid decoupling of the pressure field and the buildup of errors. The methods presented above have been used for a wide variety of heat- and mass-transfer problems,[18] as well as three-dimensional flows.[19]

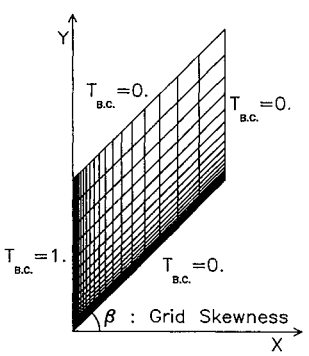

Fig. 2 Skewed and stretched grid.

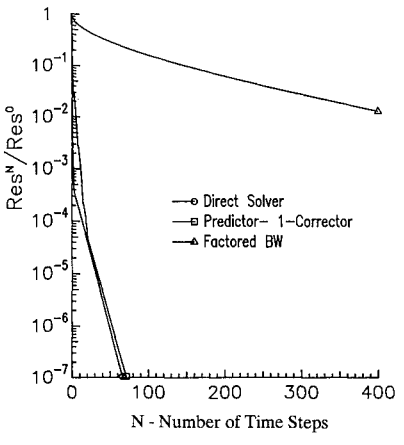

Fig. 3 Convergence history of various algorithms.

B. Continuity Equation and the Pressure Field

One of the major difficulties with the low Mach number and incompressible flow models has been the calculation of the pressure field. This difficulty is due to a little understood sensitivity of the pressure field and the convective velocity term to errors in the convergence of the continuity equation. This sensitivity seems to be much greater than in the full compressible equations, and the problem seems to be amplified further when low Mach number variable-density solutions are required. It is the present author's opinion that the problem is not one in principle, but only a practical one of sensitivity to error and poor convergence. In this article, a new method is described (the methods borrows heavily on the previous work of Chorin) and has successfully treated reacting and low Mach number flows in an efficient and time-accurate manner. The method involves two parts and these are, respectively, the solution of the continuity equation and the pressure correction at the unknown time level $(n + 1)$.

The method can be though of as a two-variable method rather than a two-grid method of the staggered-grid type, which has been used for incompressible flows in the past.[1] The staggered-grid method loses much of its attractiveness in variable-density flow due to the fact that the density must be extrapolated to the cell boundaries, and this involves an inaccuracy in the description of the mass flux into a cell volume. The present solution is to define a velocity at the cell center V used in the inertia volume term in the momentum equations, and a velocity at the cell boundaries V_b which will be used to satisfy the continuity equation and to calculate fluxes into cells. The first step of the procedure is to solve the momentum and other transport equations for intermediate values of the variables with the old pressure field. This procedure is outlined below in a typical finite-difference form, which is more familiar for most readers.

Step I—Solution of Momentum Equations with Old Pressure Field

$$\rho(V' - V^n)/\Delta t = -\nabla p^n + RHS^{n+1} \tag{9}$$

where the following notation has been used:

V' = intermediate velocity at cell center
V^n = previous velocity at the cell center
$p^{n+1} = p^n + \alpha$
RHS^{n+1} = viscous plus the convective terms at $(n + 1)$

Step II—Correction of the momentum equations with the pressure correction α to be determined from the continuity equation

$$\rho(V^{n+1} - V')/\Delta t = -\nabla\alpha \tag{10}$$

The addition of steps I and II yields

$$\rho(V^{n+1} - V^n) = -\nabla(p + \alpha) + RHS^{n+1} \tag{11}$$

which is a consistent form of the full Naiver-Stokes equations, and the overall method can be made second-order accurate in time if iteration is employed.

The pressure correction α is to be determined from the use of the continuity equation in the following fashion

Basic idea: A velocity correction at the cell boundaries will be introduced to satisfy the continuity equation, and which will determine the pressure correction during a time step. This is an alternative to having staggered grids, and it seems to be advantageous for time-dependent problems on complex grids.

The specific procedure is to form the average density and velocities at the cell boundaries and apply the continuity equation, which results in the following equations:

Integrate $\rho_b V_b$ Around the Cell:

$$\text{(I)} \qquad \iint_b \rho_b (V_b = V'_b + V_c) \cdot dA \tag{12}$$

Apply Continuity Equation:

$$\iint_b [\rho_b V_b \cdot dA] = \partial\rho/\partial t \, dV$$

therefore

$$\iint_b [\rho_b V'_b \cdot dA] = -\iint_b [\rho_b V_c \cdot dA] - \partial\rho/\partial t \, dV \tag{13}$$

where the following definitions are used:

V'_b = averaged velocity at cell boundaries obtained from step I of the momentum equations
V_b = corrected velocity at the cell boundaries after the velocity correction
V_c = velocity correction at the cell boundaries
$V_b = V'_b + V_c$
ρ_b = average density at cell boundaries obtained from the energy equation and the equation of state
ρ = density at the center of the cell
dV = volume of cell

The next step is to define a velocity potential ϕ

$$-\nabla\phi = \rho_b V_c \tag{14}$$

If the velocity comes from a potential function, then all of the rotational components of velocity come only from the momentum equations where viscosity plays its roll. The velocity potential is substituted into the continuity equation, and the following integral Poisson equation for ϕ is obtained:

$$\text{(II)} \qquad \partial\rho/\partial t \, dV + \iint_b [\rho_b V'_b \cdot dA] = \iint_b [\nabla\phi \cdot dA] \tag{15}$$

If the half cells which appear near the computation boundaries for a nonstaggered grid are included in the mass balance, there is not need to apply boundary conditions for the velocity potential ϕ (except for the downstream boundary). In general, the half cells near the wall are not treated for the transport equations, but if the half cells are not include in the mass balances, it is necessary to apply boundary conditions for the pressure correction α. The boundary conditions should be obtained from the limit of the momentum equation near the surface, or approximations related to them. The typical high Reynolds number boundary conditions for ϕ are the following, but they should be modified for specific applications.

Boundary Conditions for

Solid Wall (No Wall Mass Transfer):

$$V_c \cdot dA]_w = 0$$

or

$$\nabla\phi \cdot dA = 0 \qquad \text{or} \qquad \partial\phi/\partial n = 0 \tag{16}$$

Inflow – Constant Velocity:

$$\partial\phi/\partial n = 0 \tag{17}$$

Outflow:

$$\phi = 0 \tag{18}$$

This boundary condition can be confusing, but corresponds to the analytical condition. Also we need a value of ϕ specified somewhere on the boundaries.

The pressure correction α is obtained directly from the velocity correction potential ϕ, and the justification for this can be seen by applying the partial form of the momentum equation at the grid boundary (the same as a staggered grid).

Split Momentum Equation Applied at the Boundary of the Cell:

$$\rho_b V_c/\Delta t \, dV_b = -\iint_b \alpha_b \boldsymbol{n} \cdot dA \tag{19}$$

where the following notation is used:

dV_b = volume of hypothetical staggered grid
$\alpha = \phi/\Delta t$

Applying Gauss's Theorem,

$$\rho_b V_c/\Delta t dV_b = -\nabla\alpha_b dV_b = -\nabla\phi/\Delta t dV_b \quad (20)$$

Thus, it is seen that the velocity potential ϕ and the pressure correction α are directly related by the time step.

The above formulation of the calculation of the pressure field has the advantages that there is not any decoupling of the pressure field, the continuity equation can be solved to machine accuracy at every time step, and the method is time accurate. This combination represents an advancement over most older methods, and it accomplishes this without the complexity of a staggered grid. Another significant new feature is the use of a direct solver to calculate the velocity and pressure corrections.

C. Moving Boundaries

The final topic to be discussed in this section on numerical methods is the treatment of moving control volumes in general, and moving control volumes for vaporizing deposits in particular. For a control volume for which the boundaries are moving in time with velocity V_b, the following equation can be derived from kinematic considerations.

Moving Boundary Equation:

$$\partial/\partial t|_b [\iiint dV] = \iint V_b \cdot dA \quad (21)$$

If this result is combined with the general form of Liebnitz rule for any property s,[15]

$$d/dt|_b \iiint s dV = \iiint \partial s/\partial t dV + \iint s V_b \cdot dA \quad (22)$$

the continuity equation can be written in the moving control-volume form, which is as follows:

Moving Boundary-Continuity Equation:

$$\partial/\partial t|_b [\iiint \rho dV] + \iint \rho(V - V_b) \cdot dA = 0 \quad (23)$$

In general, all of the equations can be converted into a similar form, and the moving control-volume form has the advantage of physical clarity for the moving boundary terms when compared to the time-dependent metrics of generalized coordinates. (The number and complexity of the computations are the same.) However, this full complexity is not needed for the burning or vaporizing droplet problem, since the droplet surface is spherical and the coordinate system can be reduced with the interface in a self-similar way. If all lengths are made dimensionless with the time-dependent radius $r_o(t)$, the volumes and areas of the cells remain self-similar, and they need only to be corrected by a time-dependent term. For example, if the dimensionless length terms are denoted by a prime, the continuity equation can be written as

$$\partial/\partial t|_b [\iiint \rho dV] = \partial\rho/\partial t \Delta V' + \rho\partial/\partial t|_b [\iiint dV]$$
$$= -\iint \rho(V - V_b) \cdot dA \quad (24)$$

Since the radius of a hydrocarbon droplet is usually receding at a rate that is small with respect to the other time scales in the problem, the extra terms can be treated explicitly without influencing the numerical stability of the procedures. With the use of the direct solver for the velocity and pressure corrections, the self-similar form is essential since the lower and upper decompositions of the matrix can be made independent of the changing coordinate system.

Results

The results presented in the article will be concerned with a complet droplet burning problem, which involves the vaporization and burning of a 50-μm radius octane droplet at 10 atms. The initial conditions for the problem consisted of the injection of the droplet into high-temperature air, $Re = 100$, $T_g = 1250$K, and the initial droplet temperature was 470K. In order to simplify the calculation, the internal droplet circulation was neglected, it was assumed that the droplet temperature was uniform in space and increased in time due to droplet heating. (This is a reasonable approximation since a large percentage of the droplet mass is contained in the outer portion of the droplet.) Under these conditions, there is an initial droplet heat-up period until the total surface heat transfer is eventually consumed by mass transfer. The concentration of the fuel at the droplet surface is determined by the Clasius-Clapeyron relationship,[16] and the surface mass transfer determined by diffusion. The results will be presented so that the various flow regimes that the droplet undergoes will be illustrated. (Note: The transport properties of Ref. 16 and the single-step chemical mechanism of Ref. 17 have been utilized.)

It is instructive to begin the study with a series of snapshots of the isotherm contours around the droplet, Figs. 4–7, which illustrate clearly the influence of Reynolds number on the chemistry and flame structure. (The coordinate system has been normalized with respect to the local droplet radius and the Reynolds number is based on the local radius and relative velocity between the gas and droplet center.) The highest Reynolds number condition in Fig. 4 shows an isotherm pattern very similar to the steady-state results presented in Ref. 6. (Note: The isotherm distributions are uniform over the ranges stated in the figures.) The gas phase of the flow appears to be essentially quasisteady under the present flow conditions, and the chemistry is not fast enough to stabilize the flame on the forward portion of the droplet. As the droplet velocity decays with respect to the gas, the flame structure begins to approach the droplet in the vicinity of the well-mixed and relatively hot-separated shear layer which leaves the droplet surface. As the Reynolds number approaches 25 (Fig. 5), the flame begins to move around the droplet to the front stagnation point, and at the Reynolds number of near 20 (Fig. 6), the flame completely surrounds the droplet. The last series of temperature contours shown in Fig. 7 exhibit a very diffuse flame that is moving well ahead of the droplet into the oncoming gas flow.

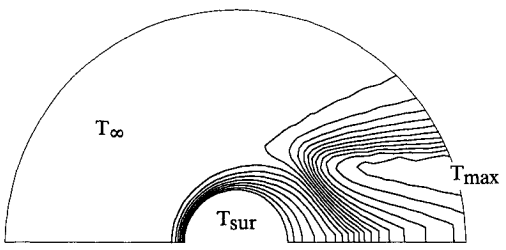

Fig. 4 Temperature contours ($Re = 49.1$; $T_s = 479$K; $\tau = 11.9$; contour range: $479\text{K} \le T \le 2412\text{K}$).

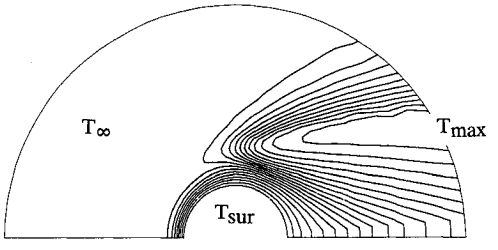

Fig. 5 Temperature contours ($Re = 31.9$; $T_s = 494K$; $\tau = 19.5$; contour range: $494\text{K} \le T \le 2438\text{K}$).

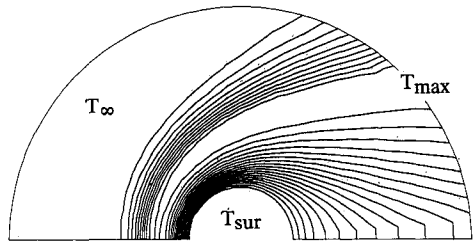

Fig. 6 Temperature contours ($Re = 22.7$; $T_s = 503$K; $\tau = 24.5$; contour range: 503K $\leq$ 2498K).

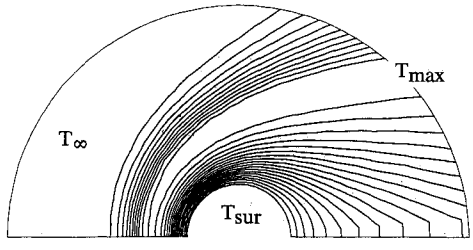

Fig. 7 Temperature contours ($Re = 18.7$; $T_s = 504$K; $\tau = 27.1$; contour range: 504K $\leq T \leq$ 2550K).

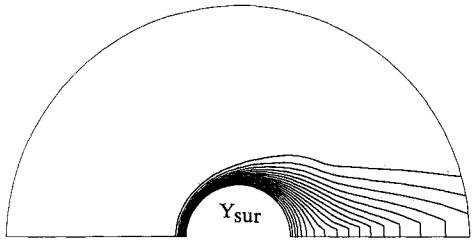

Fig. 8 Fuel contours ($Re = 49.1$; $T_s = 479$K; $\tau = 11.9$; contour range: $0 \leq Y_k \leq 0.598$).

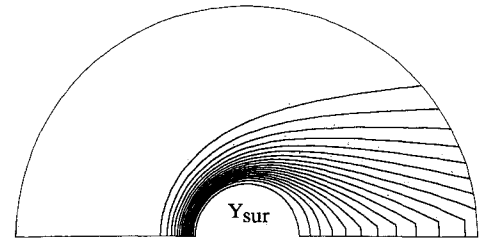

Fig. 9 Fuel contours ($Re = 18.7$; $T_s = 504$K; $\tau = 27.1$; contour range: $0 \leq Y_k \leq 0.926$).

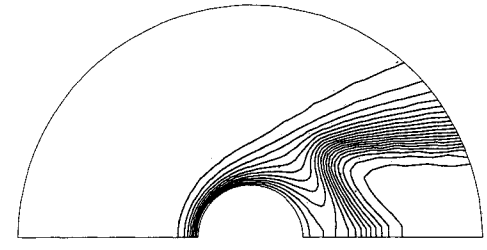

Fig. 10 Oxygen contours ($Re = 49.1$; $T_s = 479$K; $\tau = 11.9$; contour range: $0 \leq T \leq 0.21$).

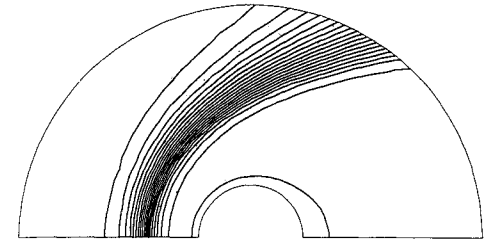

Fig. 11 Oxygen contours ($Re = 18.7$; $T_s = 504$K; $\tau = 27.1$; contour range: $0 \leq T \leq 0.21$).

The time given in all of the figures has been made dimensionless with the initial droplet radius and the thermal diffusivity of the freestream air.

The distribution of fuel mass fraction at the two extreme Reynolds numbers is shown in Figs. 8 and 9, and it is seen that the mass contours reflect the local value of the Reynolds number very closely. For the higher Reynolds number flow in Fig. 8, the fuel is limited to the boundary layer and wake of the droplet, and the largest mass fraction concentrations are reached in the wake. The opposite picture is shown by the oxygen mass fraction contours in Figs. 10 and 11, and it is clear that very little oxygen is present near the symmetry line of the wake. At the lower Reynolds number condition, the influence of the low mass-diffusion coefficient relative to heat transfer is shown in Fig. 9. This Lewis number effect in the gas phase causes the fuel mass fraction contours to be bunched near the droplet surface, and this is a direct result of the higher Peclet number.

Another potential problem with any multidimensional numerical simulation is caused by the flame approaching the upstream computational boundary of the gas flowfield at the lower Reynolds number condition. In order to avoid this problem, the physical boundary conditions of the computational zone must be extended further upstream, and the transition from the inflow to the outflow boundary condition must be further upstream. Also, from the numerical point of view, it should be mentioned again that the dynamic pressure-field calculation is very sensitive to fast chemistry through the time-dependent density term in the continuity equation. If the mass fractions begin to oscillate between neighboring cells, the pressure oscillations can become quite large, and the solutions can degrade seriously. Further studies are needed in this area to determine if the low Mach number model amplifies this problem because of the infinite sound-speed assumption that is applied.

The global characteristics of this flow as a function of time are shown in Figs. 12–15. A particular interesting characteristic is the total drag coefficient and its components, which are shown in Fig. 12. In general, the value of the drag coefficent is much lower than the standard drag curve for flow over a sphere, but the general level is predicted in an approximate way by the correlation of Renksizbulut and Haywood (entitled the RH correlation in Fig. 12.)[8] This steady-state correlation assumes that all of the heat transfer is utilized for mass transfer, and this is not true early in the droplet lifetime because of internal heating. The calculated drag coefficient is higher than the correlation due to reduced mass transfer, and the calculated results approach the correlation as the droplet temperature increases due to heating. The correlation also does not take into account the dynamic motion of the flame around the droplet, and the increase in drag coefficient during flame engulfment is not reproduced. However, in general the correlation does give a rough time-dependent average of the drag coefficient, and it can be useful in design applications. The pressure and thrust drag components shown in Fig. 12 make it quite clear that the major component of drag is being contributed by the pressure drag. The thrust drag and the friction drag (that contributed by the shear stress) are small relative to the pressure drag, and the most dramatic influence of the surface mass transfer is the lowering of the friction drag.

The Nusselt number curve in Fig. 13 does not agree with conventional results or the correlation developed by Renk-

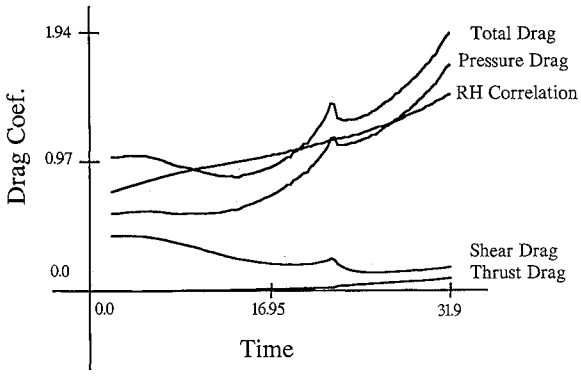

Fig. 12 Droplet drag components vs time.

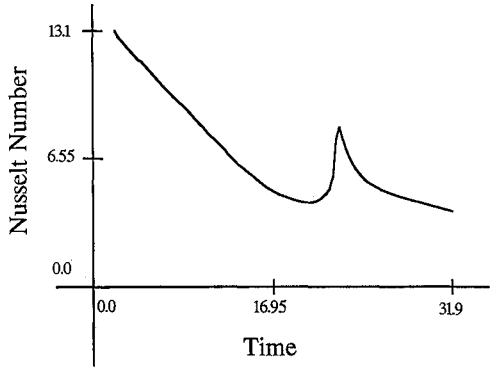

Fig. 13 Nusselt number vs time.

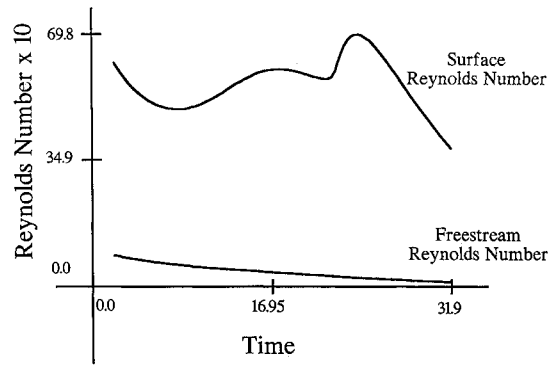

Fig. 14 Reynolds number vs time.

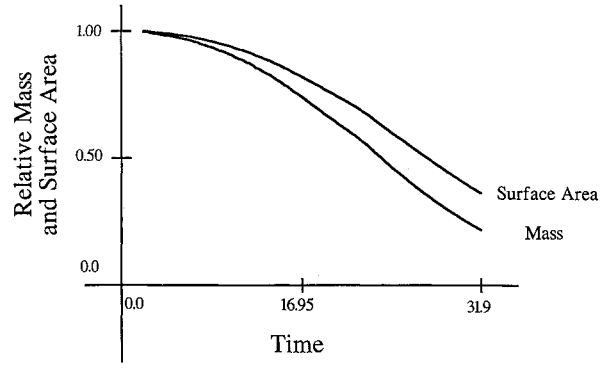

Fig. 15 Variation of droplet surface area and mass.

sizbulut,[8] due to the influence of the flame structure. The definition of Nusselt number contains the difference in temperature between the gas freestream and the droplet surface temperature, but this underestimates the potential for heat transfer caused by the higher temperatures of the chemical reactions. However, it is not a simple question of using a different temperature in the definition of the Nusselt number, such as the adiabatic flame temperature, since the flame position is changing continuously in time. As the Reynolds number decreases, the flame first contributes to heat transfer in the wake of the droplet, and then gradually heats the entire droplet as the flame envelops the droplet at lower Reynolds numbers. It is seen that there is a rather long transition in the heat-transfer processes as the flame move around the droplet, and the peak in Nusslet number is caused when the flame first surrounds the droplet. It is the opinion of the present investigators that this type of process can only be treated well with a complete numerical simulation.

The significant influence that variable transport properties can have on a vaporizing and burning droplet problem can be seen in Figs. 14 and 15, where two different definitions of the Reynolds number are presented. These two definitions are based on the gas and surface properties, respectively, and they are defined as

$$Re_g = \rho_g V_g D/\mu_g, \qquad Re_s = \rho_s V_g D/\mu_s \tag{25}$$

The surface Reynolds number given in Fig. 14 is much larger than the gas values given in Figs. 14 and 15, and this is caused by the lower temperature, higher molecular weight, and lower viscosity near the octane droplet surface. In order to use a correlation for the drag coefficient, the large density change at the surface is not important, since the inviscid flow outside the boundary layer is only influenced by the freestream conditions. However, for the interior of a droplet spray, the density change caused by cooling and high fuel concentrations could easily cause Reynolds number differences of the order shown in Figs. 14 and 15. Therefore, it appears that in many droplet flows it will be very difficult to apply semiempirical correlations because of the lack of knowledge about the flow transport properties. In order to obtain these properties, a numerical simulation seems to be required, and the numerical simulation will yield the flowfield characteristics without the need for a correlation. Also, since the capabilities of the digital computer are increasing rapidly, it will be more feasible in the future to carry out difficult calculations of this type. Therefore, it appears that simulations of the type presented in this article will play an increasing role in droplet dynamics and combustion flow systems in general.

Conclusions

The major conclusions of the present research effort have been the following:

1) A general control-volume formulation of the basic equations of mass, momentum, and energy has been developed and presented. The method reduces to generalized coordinates on a structured grid, but it has the advantageous of clear physics for all equations and boundary conditions, as well as extensions to complex cell shape.

2) A two-velocity-variable formulation of the pressure-correction algorithm for low Mach number flows has been developed and applied to reacting flows. This new method is an alternative to the use of a staggered grid and is applicable to unsteady and variable-density flows.

3) The direct solution of the pressure-correction Poisson equation has been accomplished with a banded solver of the LUD type. The banded solver is independent of the transport properties and time step, and a matrix inversion only needs to be done once for use at all time steps. The use of this technique insures that the continuity equation will be converged to machine zero at each time step, and nonlinear errors in the pres-

sure-correction algorithm will be suppressed.

4) Very fast chemical reaction rates can cause oscillations in the pressure field, and this may be caused by the low Mach number formulation itself. This subject as well as the uncertainty in chemical reaction rates should be studied more in the future.

5) For a fuel droplet starting at a high Reynolds number condition, the flow regimes can change quickly due to an interplay with the flame location. As the flame moves from the rear to the front of the droplet, there are large changes in droplet heating rates and smaller changes in the drag coefficient.

6) The general ability of the computed results to simulate droplet burning and flow seems to be good at the present time, and the future of this type of research seems to be promising.

However, there is much work left to be done on the chemical rate terms from the point of view of the numerical methods and the physical accuracy.

Acknowledgment

This research was paritally supported by Saudi National Laboratories, Livermore.

References

[1]Patankar, *Numerical Heat Transfer and Fluid Flow,* Hemisphere Publishing Corporation, New York, 1980.

[2]Roache, P., *Computational Fluid Dynamics,* Hermosa Publishers, Albuquerque, New Mexico, 1979.

[3]Chorin, A. J., "Numerical Solution of the Navier-Stokes Equations, *Mathematical Computations,* Vol. 22, 1968, pp. 745–762.

[4]Renksizbulut, M. and Yuen, M. C., *Journal of Heat Transfer,* Vol. 105, 1983, pp. 389–397.

[5]Dwyer, H. A. and Sanders, B. R., "Detailed Computation of Unsteady Droplet Dynamics," 20th Symposium on Combustion (Inter), The Combustion Institute, 1984, pp. 1743–1749.

[6]Dwyer, H. A. and Sanders, B. R., "A Detailed Study of Burning Fuel Droplets," 21st Symposium on Combustion, The Combustion Institute, 1986.

[7]Patnaik, G., Sirignano, W. A., Dwyer, H. A., and Sanders, B. S., "A Numerical Technique for the Solution of Vaporizing Fuel Droplet," *Proceedings of the 10th International College on the Dynamics of Explosions and Reactive Systems,* Berkeley, CA, 1985.

[8]Haywood, R. J., "Variable-Property, Blowing, and Transient Effects in Convective Droplet Evaporation with Internal Circulation," M.S. Thesis, Univ. of Waterloo, Canada, 1986.

[9]Steger, J.L.,"Implicit Finite-Difference Simulation of Flow About Arbitrary Two-Dimensional Geometries," *AIAA Journal,* Vol. 16, July 1978, pp. 679–686.

[10]Anderson, D. A., Tannehill, J. C., and Pletcher, R. H., *Computational Fluid Mechanics and Heat Transfer,* Hemisphere Publishing Corporation, New York, 1984.

[11]Merkle, C. L. and Choi, Y, "Computation of Compressible Flows at Very Low Mach Numbers," AIAA 24th Aerospace Sciences Meeting, Reno, NV, Jan. 1986.

[12]Dongarra, J. J., et al., *LINPACK-USER'S GUIDE, SIAM,* Philadelphia, PA, 1979.

[13]Beam, R. M. and Warming, R. F., "An Implicit Factored Scheme for the Compressible Navier-Stokes Equations," *AIAA Journal,* Vol. 16, April 1978, p. 393–402.

[14]Ibrani, S. and Dwyer, H. A., "A Study of Flow Interactions During Axisymmetric Spin-Up," *AIAA Journal,* 1987.

[15]Bird, R. B., Stewart, W. E., and Lightfood, L. N., *Transport Phenomena,* John Wiley and Sons, 1960.

[16]Abramson, B. and Sirignano, W. A., "Approximate Theory of a Single Droplet Vaporization in a Convective Field," 2nd ASME-JSME Joint Thermal Engineering Conf., HI, March, 1987.

[17]Westbrook, C. and Dryer, F. L., "Simplified Reaction Mechanisms for the Oxidation of Hydrocarbon Fuels in Flames," *Combustion Science and Technology,* Vol. 27, 1981, pp. 31–43.

[18]Soliman, M., "Solution of the Navier-Stokes Equations with Variable Density, Heat and Mass Transfer," Ph.D. Thesis, Dept. of Mechanical Engineering, University of California, Davis, CA, June 1988.

[19]Dandy, D. and Dwyer, H. A., "The Influence of Freestream Vorticity on Drag Lift and Heat Transfer," *Journal of Fluid Mechanics* (accepted for publication).